

# Electron-Induced Luminescence and X-ray Spectrometer Development: Progress Report

Jaroslava Z. Wilcox, Eduardo Urgiles, Susanne Douglas, Thomas George, Jason E. Feldman,  
Jet Propulsion Laboratory  
4800 Oak Grove Dr.  
Pasadena, CA 91109  
818-354-3556

[Jaroslava.Z.Wilcox@jpl.nasa.gov](mailto:Jaroslava.Z.Wilcox@jpl.nasa.gov)  
[Eduardo.Urgiles@jpl.nasa.gov](mailto:Eduardo.Urgiles@jpl.nasa.gov)  
[Susanne.Douglas@jpl.nasa.gov](mailto:Susanne.Douglas@jpl.nasa.gov)  
[Thomas.George@jpl.nasa.gov](mailto:Thomas.George@jpl.nasa.gov)  
[Jason.Feldman@jpl.nasa.gov](mailto:Jason.Feldman@jpl.nasa.gov)

**Abstract.** The progress in the development of a surface analysis tool based on the excitation of characteristic luminescence and x-ray spectra at ambient pressure with an electron beam is described. This instrument relies on the use of a thin electron transmissive membrane to isolate the vacuum of the electron source from the ambient atmosphere, resulting in rapid spectrum acquisition, non-destructive evaluation of surfaces, and moderate-to-high variable spatial resolution in comparison to similar portable instruments. The applications of the instrument for NASA planetary exploration include determination of surface elemental composition and identification of signatures of extinct life through correlation of x-ray and optical luminescence data. The proof-of-principle for the instrument is being demonstrated through 1) simulation of observational capabilities through electron-induced excitation of x-ray and luminescent spectra from samples of interest to geologists and exobiologists, 2) characterization of the effect of thin membranes on the properties of the excitation beam, and 3) assembly and characterization of an encapsulated prototype instrument. The x-ray and luminescence spectra are acquired and analyzed using the Environmental Scanning Electron Microscope (ESEM) and Cathodo-Luminescence (CL) spectrometer, respectively. The effect of the membrane on the electron beam is being analyzed in an SEM, and the results are correlated with the results of simulations carried out to determine performance limits and to understand the influence of membrane and atmosphere interactions on the excited spectra. X-ray spectra from metal and mineral samples were obtained without and with the membrane intersecting the electron beam. A breadboard instrument supported by a vacuum apparatus is being assembled in our laboratory.

## TABLE OF CONTENTS

1. INTRODUCTION .....	1
2. INSTRUMENT CONCEPT .....	2
3. BREADBOARD INSTRUMENT .....	3
4. CHARACTERIZATION OF THE EFFECT OF MEMBRANE .....	5
5. ESEM AND CL OBSERVATIONS .....	7
6. CONCLUSIONS .....	9
7. REFERENCES .....	10

## 1. INTRODUCTION

This paper extends the work reported at the IEEE Aerospace conference in 2001 where the concept for the so called Atmospheric Electron X-ray Spectrometer (AEXS) has been described.<sup>[1]</sup> The AEXS is a novel miniature instrument concept enabling rapid elemental analysis of samples on planetary surfaces *in situ* by energy dispersive analysis of x-ray fluorescence (XRF) spectra excited by a focused electron beam.<sup>[2-5]</sup> The initial AEXS development was funded by NASA's '98 PIDDP program.<sup>[6]</sup> A new effort that builds on the results of the AEXS developmental work while extending the application of the encapsulated source to excitation and analysis of electron-induced luminescence (Cathodo-Luminescence, CL) spectra, has been funded by NASA's '02 ASTID program.<sup>[7]</sup> In this paper, we describe our progress in the development of the AEXS instrument as well as the progress in the demonstration of the proof-of-principle for the Electron-induced Luminescence and X-ray Spectrometer (ELXS). Since both instruments rely on the use of an encapsulated electron source for photon excitation,

<sup>1</sup> 0-7803-7651-X/03/\$17.00 © 2003 IEEE

<sup>2</sup> IEEE AC paper #1138, Updated November 12, 2002

characterization of the effect of the encapsulation membrane on the transmitted excitation beam is important and described here.

The enabling component for *in situ* operation of an electron beam-based surface analysis instrument is a thin electron-transmissive membrane that isolates the vacuum within the electron source from ambient atmosphere. The impinging electrons on external samples excite x-ray and other luminescence spectra that are analyzed to determine surface elemental composition, or in the case of CL images to identify unusual formations on surface that cathodoluminescence. The CL and elemental composition information can be correlated to determine the formation origin, i.e. to determine whether it is of geological or of organic origin. Three other XRF excitation sources are available for surface composition analysis in ambient pressure: (i) radioactive alpha particle sources,<sup>[8]</sup> (ii) x-ray sources, or (iii) a focused ion beam. Electron beam excited Energy Dispersive X-ray Analysis (EDX) is a widely accepted technique for determining the elemental surface composition of samples in vacuum (for example Scanning Electron Microscopy, SEM), however it has not been previously demonstrated in ambient atmosphere due to the difficulty of generating and transmitting electron beams through the atmosphere. This paper describes our progress towards demonstrating the proof of principle of a miniature electron-beam based instrument capable of exciting fluorescent spectra from samples in ambient atmosphere.

The progress involves three parallel paths of the investigation: 1) Characterization of the effect of thin membranes on the properties of the excitation beam, 2) Assembly and characterization of a prototype electron source, and 3) Observation of samples of interest to geologists and exobiologists using electron-induced excitation of x-ray and luminescent spectra in the Environmental Scanning Electron Microscope (ESEM) and Cathodo-Luminescence (CL) spectrometer, respectively. The instrument concept is described first followed by a description of progress along each of the investigation paths.

## 2. INSTRUMENT CONCEPT

Figure 1 shows the ELXS instrument concept. The instrument consists of an electron source encapsulated by an electron transmissive membrane, an EDX detection and analyzer system, a CL detection system, and a high voltage power supply. The electron source used for our current proof-of-principle experiments is a miniature electron gun manufactured by Lexel Imaging Systems Inc., which includes a thermionic emitter and electrostatic optics to focus and accelerate the emitted electrons. The results of the simulation of the excitation characteristics and of the effect of electron interaction with the membrane and outside (Mars) atmosphere on the electron beam, suggested that the base-lined electron source produce about 10 micro Amp current and the electrons are accelerated to 10keV to 20keV energy. The transmitted electrons impinge on a sample

located outside the membrane in the planetary atmosphere where they generate characteristic CL and x-ray fluorescence. The electrons also ionize the planetary atmosphere, ensuring a return current path.<sup>[9]</sup>

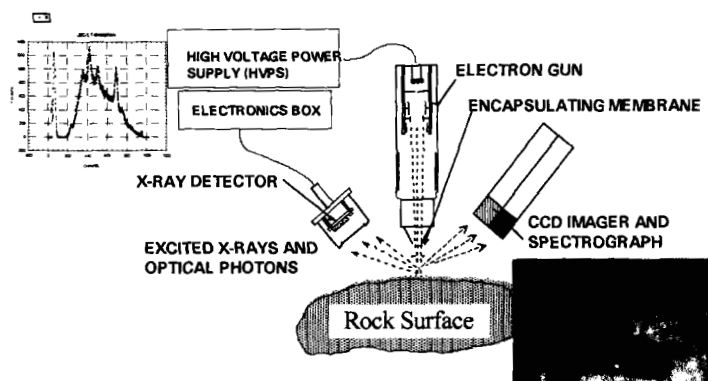


Fig. 1. ELXS instrument concept consisting of an encapsulated electron gun and X-ray and CL detectors.

Shown in the insets in Figure 1 are examples of information typical for the observational techniques incorporated into the instrument. In the upper left corner is an EDX spectrum that has been collected in our laboratory using a breadboard instrument set-up. The setup had the electron source integrated into a vacuum chamber that was interfaced with an exit window. The window had the electron-transmissive membrane incorporated into the window rim, and the whole assembly was supported by a high vacuum pump. The particular spectrum shown was obtained for a Mars composition simulated sample JSC-1. The x-ray detector was a silicon *p type-intrinsic-n type* (PIN) photodiode based system manufactured by Amptek Incorporated and used on the Mars Pathfinder Alpha Proton X-ray Spectrometer APXS<sup>8</sup> instrument. The elemental composition was determined by analyzing the excited XRF using the EDX analyzer system. In the lower right corner is shown a CL image obtained for a tufa (calcium carbonate) sample colonized with a bacterial community. The image was obtained in a commercial CL spectrometer at George Washington University (GWU).<sup>[10]</sup> Differences in the color in the image have arisen from differing mineralogy in the sample. We plan to perform and correlate CL and EDX measurements for the same samples to obtain characteristic signatures for samples of interest to geologists and exobiologists.

The use of electrons for CL and X-ray excitation enables a new approach for *in situ* XRF measurements. In the past, XRF instruments have proved to be invaluable for determining the elemental makeup of the surface of a planetary body. To date, all *in situ* missions, including Surveyor, Viking 1, Viking 2, Mars Pathfinder, and the Soviet Venera/Vega missions have carried some form of XRF instrument. XRF instruments are also being considered for future Mars missions. Previous XRF instruments have used radioactive sources to excite x-rays from planetary materials. A comparison of the AEXS, an x-

ray excitation based XRF instrument, and the Alpha Proton X-ray Spectrometer (APXS) is shown in Table 1.

**Table 1.** Comparison of salient features of portable x-ray instruments of interest to planetary scientists. While the AEXS/ELXS is comparable in mass (approximately 1 kg, not shown in the table) with the other instruments, it offers two potential advantages: short spectrum acquisition time and improved spatial resolution. A consequence of the short spectrum acquisition time is that the energy expended by the instrument per acquired spectrum is also considerably less than for the other techniques.

Property	Electron-induced excitation	XRF/XRD (proposed)	APXS (flight) <sup>[8]</sup>
Excitation particles	Electrons	x-ray photons	$\alpha$ -particles
Particle rate	$6 \times 10^{13}/s$ ( $10 \mu A$ )	Primary current: 0.3mA; X-ray photons: $2 \times 10^{12}/s$	$2 \times 10^9/s$ (50mCi)
Power	5 W (peak)	13 W	0.34 W
X-ray photons/second	$> 2 \times 10^4$	$10^2$ to $10^3$	$\sim 1$
Spectrum acquisition time <sup>(2)</sup>	<b>&lt; 1 minute</b>	5 minutes	10 hours
Energy per acquired spectrum	<b>50 J</b>	5,000 J	10,000 J
Spatial resolution	Controlled: $mm^2$ – $cm^2$ by focusing and varying the working distance	$\sim 4 cm^2$ (at 2 cm working distance)	$\sim 20 cm^2$

**Variable ( $mm^2$ – $cm^2$  scale) spatial resolution** arises due to the focusing ability for the electron beam. The small spot size will be particularly effective when used in conjunction with imaging systems. Electron interaction with the membrane material spreads the initially pencil beam into a cone angle whose width depends on membrane composition and thickness, and on electron energy. Thus the irradiated spot size will increase with increasing working distance (the distance between the membrane and interrogated sample). Using a relatively large working distance (cm-scale on Mars) the instrument could be used for surface reconnaissance. When an area appears interesting, the instrument head could be brought close to the surface for a more detailed inspection. X-ray and CL spectra would be acquired while the head steps to produce surface maps. This possibility of varying the spatial resolution is important for astrobiological investigations where large area contextual information is obtained prior to performing a higher resolution analysis. **Rapid spectrum acquisition** is needed to use the high-resolution capability. Short spectra collection times are enabled due to the combination of a large flux of the excitation particles and a one-step excitation process, leading to spectra acquisition times less than 1 minute for a  $10 \mu A$  beam (as compared to 10 hours for APXS). Such short acquisition times will also result in **low energy consumption** per spectrum and thus enable multiple readings assessing sample heterogeneity. **Short penetration depth** ( $\mu m$ -scale) for the electrons will allow surface coatings and weathering rinds on rocks to be studied with minimal mixing effects from deeper material. Measurements of unaltered surfaces will require prompt sampling of freshly cored or broken rocks, activities that are planned in several future Mars sampling missions.

### 3. BREADBOARD INSTRUMENT

The approach to demonstrating a proof of concept of the AEXS has been through assembling and operating setups with the same components as in Fig. 1 with supporting equipment. The first setup that was assembled in our laboratory is shown in Fig. 2. It consisted of a vacuum chamber that had the electron gun incorporated into it. The

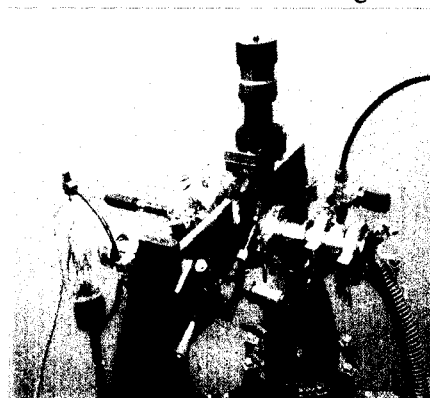


Fig. 2. AEXS laboratory apparatus mounted on a turbomolecular pump (not shown).

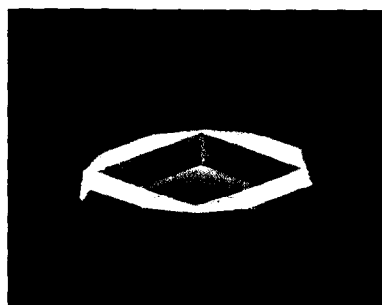


Fig. 3. SEM of a SiN membrane etched into a silicon frame.

chamber vacuum was maintained at approximately  $10^{-6}$  Torr using a turbomolecular pump. The encapsulation membrane was integrated into the chamber window through which the electron beam was transmitted into the outside atmosphere. Fig. 3 shows the membrane inside a

Si support frame. The membrane is a 200 nm thick film of Silicon Nitride (SiN) grown using low pressure chemical vapor deposition under non-stoichiometric, silane rich conditions to produce a low tensile stress, pinhole free film on both sides of a 400  $\mu m$  thick silicon wafer.

The window openings (1.5 mm x 1.5 mm) are defined by standard photolithography and reactive ion (RIE) and wet chemical etching. The frame was attached to a stainless steel flange using Epotech type H20E silver epoxy in the first setup.

Fig. 4 shows a setup that has recently been constructed as the next step towards the construction of a portable instrument. The setup consists of a commercial gun shown in Fig. 5, encapsulated with the SiN membrane. At the present time, the setup is supported also by a high vacuum pump; the connection



Fig. 4. Encapsulated gun in the present apparatus.

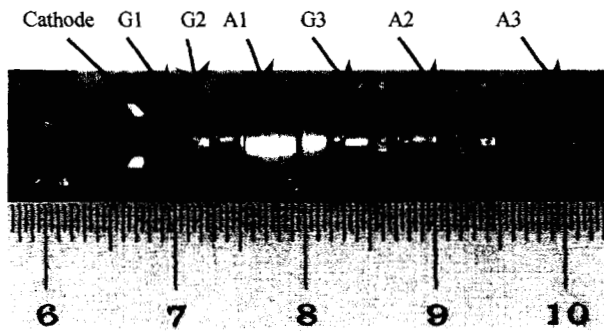


Fig. 5. Cross-section of the electron gun

between the gun and pump will be cut after the gun has been evacuated and the Pyrex evacuation port is flame sealed. To encapsulate the gun, the critical process consists of hermetically joining dissimilar materials. The gun employs lead-glass (Type L-29) envelope around its components as is common for many TV tubes or CRT's. The coefficient of thermal expansion (CTE) of Si is on the order of 3ppm whereas for the L-29 glass it is 80-90ppm, requiring a graded seal glass tubing to be inserted between the gun and the membrane. We manufactured a glass tubing transition region where approximately 10 thin rings of different glass types with progressively smaller CTEs are glass-blown together. The graded seal allows us to transition from the L-29 glass to Pyrex whose CTE is near 3ppm. Pyrex has been also selected due to its ability to anodically bond to silicon. Fig. 4 shows the gun transition region joined to the Pyrex-T, and encapsulated with an anodically bonded Si chip. Anodic bonding requires complete flatness of both surfaces and no particles in the bonding area. In Fig. 4, the encapsulated gun is shown mounted to a vacuum processing station in order to process the tube and exhaust the residual gases from the vacuum envelope. Once an adequate base pressure has been reached the tube will be pinched-off by flame sealing the exhaust tubing at the Pyrex T and the active getters will be

flashed & activated, resulting in a self contained encapsulated gun.

The x-ray spectra are acquired using a Si PIN diode detector cooled to 255K, a shaping amplifier, a multi channel analyzer (MCA) to count and sort the pulses into the proper energies, and a computer attached via RS-232 to acquire and analyze the data. The setup in Fig. 2 was used to obtain x-ray spectra for metal samples using a 10 keV electron beam and a 2 mm working distance in one atmosphere of pressure. The irradiated spot size was between 0.5 mm and 1.5 mm, and the analysis time was as short as 100 seconds. Fig. 6 compares the spectra taken in the setup for Ti with that obtained in the SEM. Note that the two clearly discernible peaks (Ti  $K\alpha$  and  $K\beta$ ) in Figure 6b are observed as a single, slightly shifted peak with a small shoulder in Figure 6a. The peaks are better resolved in the SEM due to the greater sensitivity of a liquid nitrogen (77K) cooled x-ray detector. The AEXS x-ray detector is cooled with Peltier cooling to 255 K, with the best obtainable x-ray peak width being approximately 250 eV.

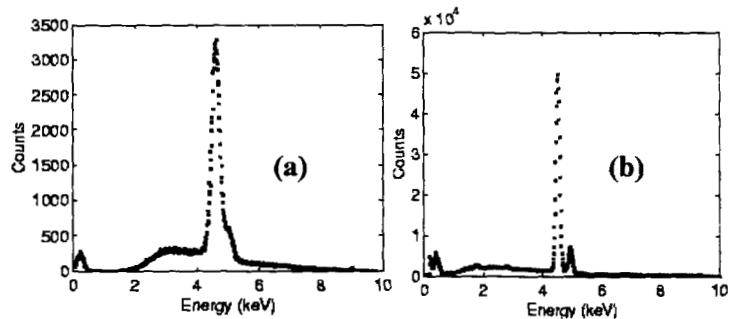


Fig. 6. X-ray spectra obtained from a pure Ti target (a) in air by the AEXS setup and (b) in a SEM operated at 10 kV. The two Ti peaks seen in (b) at about 4 keV are not completely resolved in (a) due to the poorer resolution ( $\sim 250$  eV) of the x-ray (Amptek) detector. The background counts are also higher in (a) due to the increased scattering of the electrons primarily by the membrane.

Spectra for pure targets similar to Fig. 6 were also obtained using the encapsulated gun in Fig. 4. The setup was also used to obtain spectra for several standard alloys and minerals, and JSC-1 sample. To facilitate the determination of the effect of the membrane and outside atmosphere, the spectra were acquired also in (a) SEM using the EDS detector without and with the intervening membrane, and (b) in SEM with the intervening membrane and using the same Amptek detector as for the encapsulated gun in the ELXS setup. The spectra for a Waspaloy standard (about 59%Cr, 19% Ni, 12% Co, 4% Mo, 3%Ti) are compared in Fig. 7. Note that Figs. 7a and 7b exhibit X-ray transition lines at the same locations (as they should) in all cases. Line-width broadening is observed in Fig. 7b due to the poorer resolution of the Amptek detector, increased background due to the increased scattering of the electrons by the intervening membrane and the outside (760 Torr) atmosphere. Si lines observed in the presence of the membrane are generated by electron interaction with the membrane and the membrane (Si) rim. The weak peak in

Figure 7b in the SEM experiment without the intervening membrane at about 8 keV was associated with Cu and explained in terms of geometrical reflections between the sample and the SEM enclosure. The spectral fidelity depends strongly on mutual position of the detector, target and the gun. The goal of the ongoing geometry optimization effort is to minimize the effect of the membrane presence on the spectra. An environmental chamber to house the encapsulated gun and samples within a controlled atmosphere is being assembled. The results of our modeling effort indicate that the spectra will be affected by the 7 Torr much less than by the Earth atmosphere.

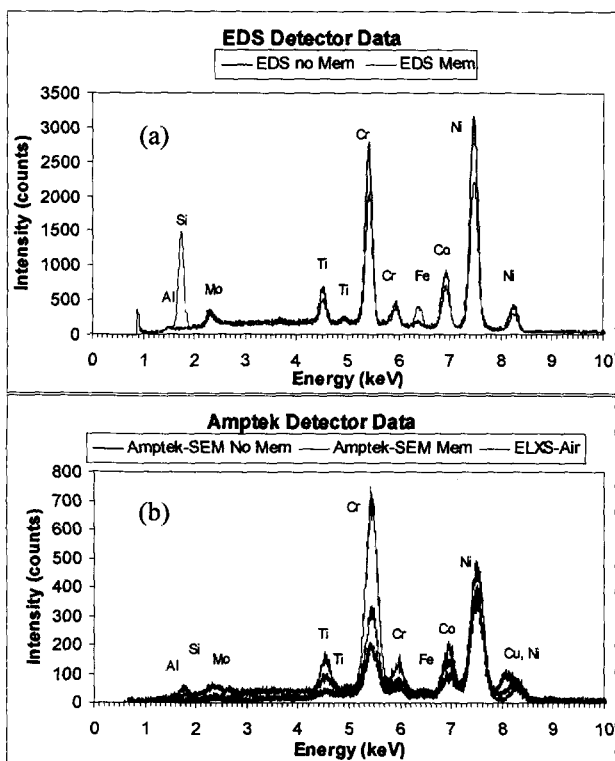


Fig. 7. X-ray spectra obtained from a Waspaloy (about 59%Cr, 19% Ni, 12% Co, 4% Mo, 3%Ti) standard. (a) in SEM without and with the intervening membrane using EDS detector, (b) in SEM and ELXS setup using the Amptek detector using .10 kV electron beam. All peaks occur at their correct locations, Si peaks occur due to electron-membrane window interaction, and lines in (b) are broadened due to the poorer resolution of the detector.

#### 4. CHARACTERIZATION OF THE EFFECT OF MEMBRANE

The membrane properties were investigated in detail due to its critical role in the encapsulated instrument. A series of experiments determined that the 1 mm x 1 mm membrane is capable of isolating high vacuum, is able to withstand differential pressure in excess of one atmosphere, survive vibrational shocks of a magnitude to be expected during a planetary mission, and have high electron transmission. The properties of the transmitted electrons through the

membrane and atmosphere are modified due to electron interaction with the molecules of the traversed medium. To determine the effect of the transmission on the excited spectra, characterization studies were performed that consisted from 1) Electron beam spreading modeling and measurements, and 2) Comparison of the excited x-ray spectra in vacuum without and with the intervening membrane. The effect of the transmission was simulated using a Monte Carlo code for transmission through multiple layers. The transmission and beam spreading were measured in SEM.

##### 4.1. Electron beam spreading studies.

Three effects of particular importance to ELXS capabilities are: 1) The fraction of the transmitted electrons, 2) beam spreading, and 3) loss of the electron energy. Electron transmission through membrane and atmosphere was

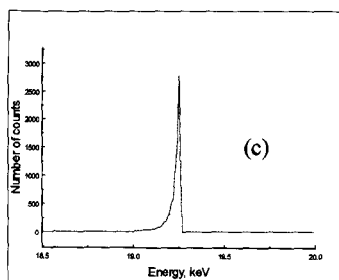
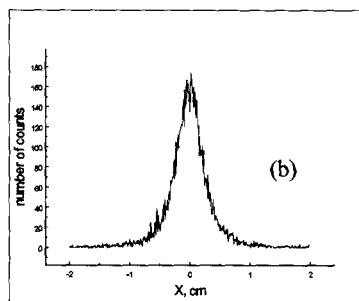
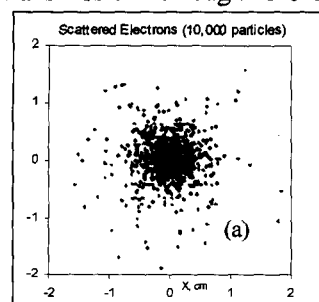


Fig. 8. Simulated distribution for 20keV electrons scattered by the interaction with a 200nm SiN membrane, at a 2mm distance from the membrane in vacuum (a, b) spatial, (c) energy distribution.

modeled using Monte Carlo simulations<sup>3</sup> of scattering events as a function of the working distance, i.e. the distance between the membrane and target. The attenuation and loss in the electron energy are due to inelastic collisions with the membrane atoms; the scattering is due to elastic collisions. Figs. 8a and 8b show an example of the simulated angular distribution for a pencil beam that has been transmitted through a 200nm thick SiN membrane, at a 2mm distance from the membrane. Note that the electron density peaks at the beam center. Figure 8c shows the spectral distribution. Note that the distribution peaks at one value of the transmitted energy corresponding to forward transmitting electrons.

The simulation results are summarized and compared with the experimentally determined spot size

(beam cross-sectional area) as a function of the working distance in Fig. 9. The simulations were performed using two models for electron scattering. The first uses conventional formulas<sup>[11]</sup> for interaction of high-energy

charged particles with matter, the second uses modified formulas following low energy electron-beam lithography.<sup>[12]</sup> The experimental beam width was determined in two ways: 1) by measuring electrical current in "knife edge" response measurements, and 2) by collecting x-ray spectra that were excited from a Si wafer that was half-coated with Ti (Fig. 10). The experiments were performed in SEM using the spot mode with the membrane inserted into the beam path, by translating the knife edge stage horizontally in the perpendicular direction to the knife edge (or to the Si-Ti boundary during the x-ray collection experiment), with similar results obtained in both cases. Fig. 11 shows a typical response for Ti counts.

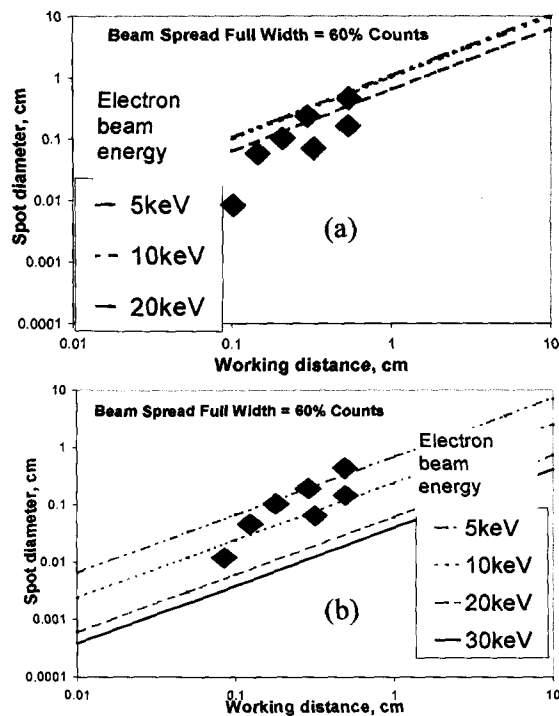


Fig. 9. Electron beam spreading (a) original, (b) modified scattering formulas following low energy lithography. Diamonds are the experimental results.  $\blacklozenge$  = 20keV,  $\blacklozenge$  = 10keV.

The scattering events depend on electron energy, membrane and atmosphere composition and thickness. For 20keV and 10keV energies, the results of the simulations using the two models differed little in the fraction of the transmitted electrons, however the beam spreading differed by a fractional amount that increases with electron energy decreasing. For example, for 20 keV electrons at a 1 mm working distance in Fig. 9, the predicted irradiated spot diameter is .6 mm and 0.06 mm using the conventional and modified formulas, respectively. The measured sizes were in-between these two values; e.g. the measured values were 0.1 mm at a 1 mm distance for 20 keV electrons, and 0.4 mm at a 1.5 mm distance for 10 keV electrons. Note that the spot size was defined here as the arithmetic average of

distances from the beam center at which the electrons impinge on the sample. By assuming a Gaussian distribution for the scattered particles for an originally pencil beam, it is easy to show that the arithmetic average corresponds to ~ 60% of the original particles in a bucket bounded by the arithmetic average radius. By assuming a Gaussian distribution for the scattered electrons, simulations of the knife edge (or x-ray yield in the wafer) experiment yield a response function (the inset in Figure 10) with the interpolated slope from the curve center that intercepts the horizontal axis at a distance equal to the arithmetic average distance. Hence the predicted spot size corresponds to the interpolated intercept in our experiments.

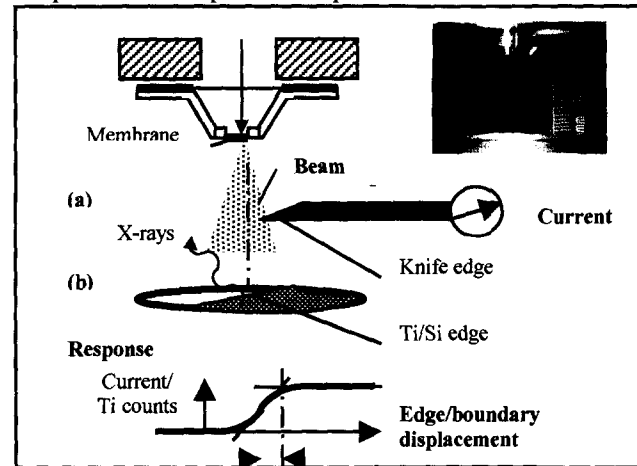


Fig. 10. Beam spread measurements in SEM (a) Knife edge, (b) Ti x-ray counts

One of the desired capabilities of an *in situ* instrument is to generate elemental composition maps for interrogated surfaces. To interpret the collected data in terms of relative abundance of the detected elements, a geologist will need to correlate the traversed distance with the number of the excitation particles. The number of the excitation particles within a circular area can be obtained by integrating the distribution function within the area. For example, an area bounded by a radius equal to twice the arithmetic average radius will bucket 80% of the scattered particles. The typical spot size shown in Fig. 9 ranges from several hundreds of micrometer to several mm. Should a smaller irradiated spot size become desirable, the spot size can be reduced by using small an external magnetic lens. For efficient focusing, the focused electrons should all have the same energy. Figure 8c showed the spatial distribution for the energy of the transmitted electrons. Note that the energy peaks at the beam center, corresponding to least interaction with the membrane. Thus a magnetic lens can be designed to perform efficient post-membrane focusing.

#### 4. 2. Elemental composition studies with and without the membrane.

To determine the effect of the membrane on the collected luminescence spectra, we have collected x-rays without and with the intervening membrane for several targets. Figure 12 shows the collected spectra for feldspar in SEM. Note that the spectrum with the membrane present shows an increased peak at Si energy line. Similar observations were made for other targets, suggesting that the increase in the Si counts is associated with the Si in the SiN membrane. The peak height will depend on mutual geometry of the membrane, target and detector; the peak count will be minimized when no x-rays with the membrane origin reach the detector entrance aperture.

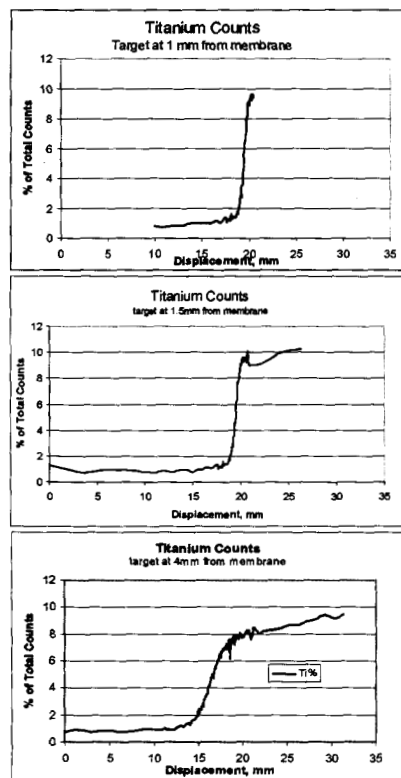


Fig. 11. Normalized Ti counts as a function of the horizontal displacement for the wafer

## 5. ESEM AND CL OBSERVATIONS

Parallel to the electron gun development, environmental scanning electron microscopy-energy dispersive spectroscopy (ESEM-EDS) and CL measurements were performed to demonstrate the ability to discriminate between biotic and abiotic sample fractions. This work consisted from 1) Selection of samples for test measurements, 2) Taking images and elemental maps of the samples using ESEM-EDS, and 3) CL imaging and preliminary CL spectra.

*Test samples selection.* The test samples ranged in age from modern endolithic ("rock-dwelling") microbial communities that were still living on collection to ancient (2.1 billion year old) fossilized communities. The basis for selection was to have samples in which the "biotic" parts have an intimate association with the mineral matrix and exhibit a range of structural preservation so that we could trace the CL signatures back in time to see if they persist. The samples were hand palm-sized cross-sectioned rocks with layered microbial communities, with no coating or other specimen preparation performed:

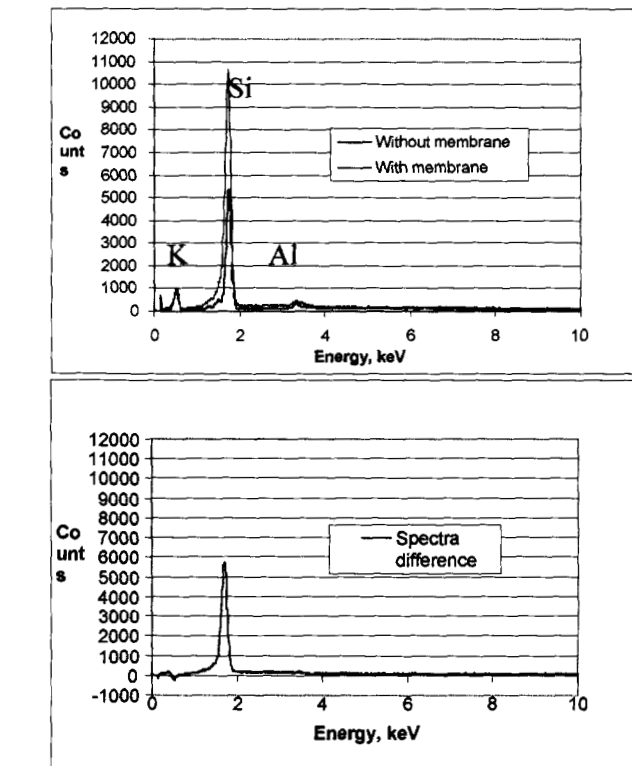


Figure 12. Feldspar spectra (a) without/with the intercepting membrane (b) spectra difference.

1. Gypsum ( $\text{CaSO}_4 \cdot 2\text{H}_2\text{O}$ ) evaporite community from Badwater, Death Valley, California. The sample consisted of an approximately 8 cm thick crust of gypsum in which coloured layers, formed by different type groups of microorganisms could be seen. from top to bottom these were: green (dominated by cyanobacteria and diatoms), pink (due to purple sulfur bacteria), and grey/black.
2. Endolith--containing tufa, a deposit of calcareous minerals from Mono Lake, California. The microbial community was observable as a thin green line approximately 5 mm under the rock surface.
3. Pumice (a silicate rock containing numerous voids due to gas inclusions) from Mono Lake shore near Lee Vining, California. The location of the microbial community was visible as a thin green line approximately 5 mm below the exposed rock surface.
4. Microfossil-containing chert from the Gunflint Iron Formation, Northern Superior, Canada (age approximately 2.1 billion years).
5. Carbonate bioherm (stromatolite) from the Ridge Route Formation in southern California (age approximately 50 million years).

*ESEM images and elemental maps* were collected with the field emission electron gun, 20keV acceleration voltage, at 7 Torr using a backscattered electron detector, which identifies microfossil areas as dark areas in the images due to a higher content of low Z elements. The Princeton-Gamma Tech energy dispersive X-ray spectrometer was optimized for light element detection with 50eV spectral

resolution, and the composition relative atomic proportions can be determined within an error margin of 0.1%.

For all the modern endolithic communities examined the presence of the microbial community within the host rock was accompanied by a distinct change in texture and appearance. In non-colonized regions, the crystal shape of the constituent mineral grains could be clearly seen (i.e., were clean and smooth on a sub-micron scale) and were representative of the particular mineral type. In the regions colonized by microorganisms the mineral grains looked "corroded" with numerous pits, crumbled surfaces, and jagged, indistinct edges (Fig. 13). The actual position of the microbial community was discernable as a "coating" on the mineral surface with occasional filamentous organisms distinguishable. This coating consisted of numerous microbial cells in close spatial proximity covered in extracellular polymers (EPS), a typical characteristic of biofilm or mat communities (Fig. 13). The EPS also enclosed small mineral precipitates which were formed as a result of microbial activity; either indirect physicochemical weathering due to microbe-induced chemical changes in the microenvironment and/or nascent precipitates formed biogenically.

The textural differences were paralleled by differences in elemental composition, both in terms of relative proportion and segregation of particular elements to specific structures. In general, the regions colonized by microorganisms had a measurably different suite of elements than the host rock (Fig. 14). The EDS results are presented as "atom %" (abbreviated simply as "%"). Thus they represent a percentage, in terms of the number of atoms present for all the inorganic elements measured. It should be noted that analyses ascribed to "cells" were done on structures which were unmistakably microbial (i.e., filamentous or of exopolymer-covered cell aggregates; use of ESEM allowed these to be identified as "wet" so that it was more than a morphology-based identification). Those ascribed to the "mineral" category were from mineral grain faces that appeared flat and clear of small protrusions as seen at sub-micrometer resolution and of which the three-dimensional crystal shape could be clearly seen. Therefore we are confident that our results show real differences between the mineral and microbe portions of our sample. (During the spot mode EDS analysis of the microbial structures, the ESEM water vapor pressure in the chamber increased, showing that the sample contained water. This did not happen when mineral grain faces were examined, providing additional evidence for biological origin. Shape alone, especially by purely topographical techniques such as SEM, although powerful, is not sufficient for identification of a

sample as being of biotic or abiotic nature.) No beam damage was seen to occur to the specimen, which would indicate that the beam may be penetrating through or destroying the sample.

ESEM-EDS analyses of the fossilized microbial communities showed that there were significant differences in elemental composition between the microfossil-containing regions and the host rock (Fig. 15). For the 2.1 billion year old Gunflint sample, the microfossil regions had



Fig. 13: ESEM images of the endoevaporitic microbial community from Death Valley showing effects of microbial presence on mineral texture. The left image shows the transition zone between uncolonized gypsum (bottom) and colonized gypsum. In the uncolonized zone, the gypsum crystals have smooth faces and sharp edges. In contrast, crystals in the colonized zone appear pitted and corroded (C), where the biofilm (B) has effected gypsum dissolution. The right image shows an overview of the biofilm (B) draped over gypsum crystals in the colonized zone of the crust.

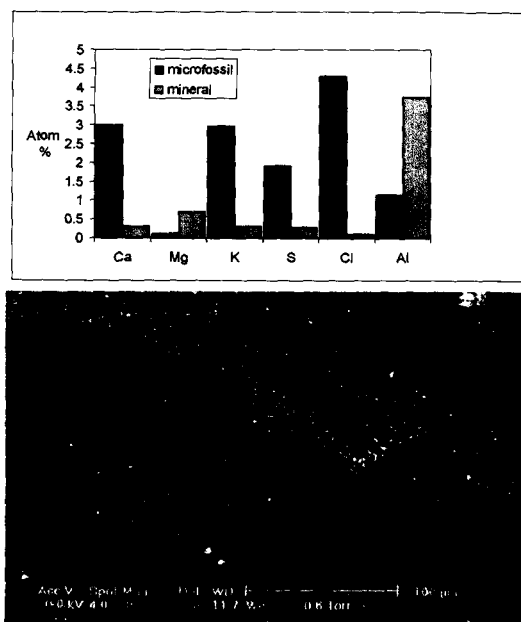


Fig. 14: EDS spectrum and backscattered electron image of the 2.1 billion year old Gunflint Iron Formation. There is a marked contrast in elemental composition between the microfossil region (dark band in image) and the host rock. The areas from which spectra were collected are indicated by appropriately colored stars in the image.

elevated levels of Fe, C, Cl, S, and Ca while the background host rock matrix simply contained Si and O. Therefore this approach is useful for discriminating between biotic and

abiotic regions in a host rock and serves as a direct analogy for our ELXS technology. CL measurements, made on the same samples, should provide corroborative information showing differences between the biotic and abiotic sample portions.

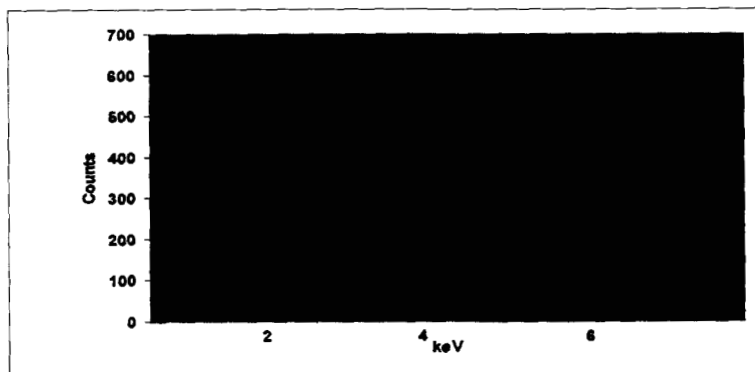


Fig. 15: EDS spectrum for cells vs. mineral in the Death Valley sample. A multitude of elements are typical of the cellular composition while the mineral, gypsum, gives only Ca and S. The high Si content is typical for the groundwater in the area.

CL images and spectra are being collected at the present time. Fig. 16 shows a preliminary result that shows that differences in mineralogy are reflected as different colors in the images. Thus we are able to note mineralogical variation in a sample and use this information for subsequent analytical measurements. The spectral capabilities of our CL instrument have just recently become operational and plan to continue those experiments to verify the utility of correlated measurements for planetary observations.



Fig. 16: CL image of the colonized tufa (calcium carbonate) from Mono Lake, CA exhibits color differences arising from differing mineralogy. The carbonate matrix (C) is seen here to have a rough surface with crevices such as the one shown here. Within the crevice, a microbial biofilm (B) has cemented together numerous mineral grains of differing types. The width of the sample shown in the image is approximately 5 mm.

## 6. CONCLUSIONS

In summary we have embarked on an effort to develop an electron-based instrument for observation of planetary surfaces in situ. In situ observation in planetary atmospheres is enabled through using a thin electron-transmissive membrane for vacuum-isolation of the electron source. The electrons accelerated in the electron column to 10keV-20keV, are focused and transmitted through the membrane on samples in ambient atmosphere where they excite characteristic x-ray and CL luminescence from the irradiated spots. The proof-of-principle experiments performed in our laboratory to date include 1) acquisition of spatially resolved x-ray spectra of samples in air by using a breadboard setup, 2) beam spreading measurements in SEM to determine the spatial resolution and performance limits for the proposed instrument, and 3) ESEM-EDS and CL characterization of samples of interest to planetary geologists and exobiologists using standard laboratory equipment. In addition, as the next step towards the construction of a portable electron source, we are proceeding to encapsulate a commercially available electron gun and evacuate it using our laboratory station.

Using a 10 keV electron beam and a 2 mm working distance in one atmosphere, we have obtained x-ray spectra from pure metal and JSC-1 samples using 10 keV beam, with the analysis time as short as 100 seconds. We have determined that the spot size irradiated by the transmitting electrons through a 200nm thick SiN membrane is on the order of several hundreds micrometers to several millimeters, depending on the electron beam energy and the working distance between the membrane and target. Our models predict that the spatial resolution and beam transmissivity will be improved by increasing the energy of the irradiating electrons, by reducing the working distance, and by working in reduced atmospheres such as Mars ambient. In Mars atmosphere (approximately 7 Torr) a 25 keV beam has been predicted<sup>3</sup> to resolve areas as small as 100  $\mu\text{m}$  at 2 mm working distances, thus offering the potential for a compact instrument for performing rapid in-situ surface analysis at medium spatial resolution. We expect this new analysis tool to find its place among other ambient pressure surface analysis systems. Techniques such as X-MIBA provide focused beams for surface analysis with spatial resolutions as small as several square  $\mu\text{m}$  but require large stationary instruments. Commercially available portable instruments, such as the MCA-4000 analyze surface regions of dimensions of several square centimeters.<sup>[13]</sup> The potential for miniaturization and the spatial resolution of the encapsulated electron beam-based instrument fills the gap between non-portable, high resolution laboratory instruments and portable, low resolution in situ instruments such as the APXS used in the 1997 Mars Pathfinder mission. Additionally, examination of CL images shows that a correlation with x-ray spectra exists, suggesting that

by collecting both spectra an additional insight into the nature of interesting formations on target surfaces could be obtained.

## 7. REFERENCES

- [1] J.E. Feldman, J.Z. Wilcox, T. George, N. Bridges, "Atmospheric Electron X-ray Spectrometer Development", paper presented at IEEE'01 conference, and reprinted in the conference proceedings.
- [2] T. George, "Miniature Electron Microscopes without Vacuum Pumps", NASA Tech Briefs, NPO-20335, Aug. '98.
- [3] J.Z. Wilcox, "Simulation of Transmissivity of Electron Beam in Mars Atmosphere", JPL Internal Document, 1997.
- [4] J.E. Feldman, T. George, and J.Z. Wilcox, "Atmospheric Electron X-ray Spectrometer" US Patent # 09/390,547; filed 9/3/99.
- [5] J.E. Feldman, J.Z. Wilcox, T. George, D. Barsic, and A. Scherer, "Elemental Surface Analysis at Ambient Pressure by Electron-Induced X-ray Fluorescence", accepted for publication by Rev. Sci. Instr., 2002.
- [6] J.Z. Wilcox, T. George, J.E. Feldman, N. Bridges, C. Hansen, "Atmospheric Electron X-ray Spectrometer Membrane Viability", a funded proposal by NASA's '98 PIDDP program.
- [7] J.Z. Wilcox, T. George, S. Jurewicz, A. Chutjian, J. Hanchar, "Electron Induced Luminescence and X-ray Spectrometer Development", a funded proposal by NASA's '01 ASTID program.
- [8] Rieder R, Wanke H, Economou T, et al., "Determination of the chemical composition of Martian soil and rocks: The alpha proton X ray spectrometer," J. Geophys Res-Planet 102: (E2) 4027-4044 FEB 25 1997
- [9] G. D. Danilatos, *Scanning* 4, 9 (1981); Adv. Elect. & Elect. Phys. 71, 109 (1988); E.D.H. Green, "Atmospheric scanning electron microscopy", PhD dissertation, Dept. El. Eng., Stanford Univ., (1992)
- [10] Courtesy of Dr. J. Hanchar, George Washington University, Washington DC.
- [11] D. Joy, "Monte Carlo Modeling for Electron microscopy and Microanalysis," Oxford University Press, 1995.
- [12] R. Browning, T. Eimori, E.P. Traut, B. Chui, and R. Pease, V. Vac. Sci. Technol. B, Vol. 9, 3578 (1991).

- [13] B.L. Doyle, D. S. Walsh, and S. R. Lee, Nucl. Instrum. and Methods in Physics Research

**Jaroslava Z. Wilcox** is a Senior Technical Staff member at the In situ Technology and Experiments Systems Section at JPL. She is a co-inventor with T. George and J. Feldman of a miniature ring

orbitron ion pump for electron microscope applications as well as the AEXS concept. She received her PhD in Solid State Physics at the University of California at Los Angeles,

taught at Tufts University for two years, after which she joined TRW Space Systems where she worked in the area of millimeter-wave imaging, a novel phased array SAW RF spectrum analyzer, and mostly, in electro-optics: She was the principal investigator of QWIP IR sensors program, was the program manager of the program for the development of GaAlAs solar cells, and a task leader for several diode laser development programs. She designed and analyzed performance of MQW diode lasers and arrays of diode lasers for coherent emission and pumping solid state lasers. Dr. Wilcox joined JPL in 1990, where she participated in the development of the vibrational micro-gyroscope and other MEMS devices. She was involved in the calibration of the evolved water experiment for DS2 New Millennium (NMP) mission. Her current activities involve NMP support and research in the area of micro-instruments for in-situ observations. She received several technical achievement awards, was listed in "American Men and Women in Science" and "Who is Who in Technology Today", has published over 95 papers in refereed journals, has given several invited and numerous contributed talks at professional meetings, and holds several patents in the area of solid state devices.



**Eduardo Urgiles.** Ed is a JPL contractor with practical experience in setting up lab equipment, semiconductor processing, instrument data acquisition, and building and maintaining high vacuum systems. Ed graduated from California State University at Los Angeles in 1996. He was a research fellow at the National Renewable Energy Lab, Golden, Co, where he conducted projects in semiconductor and superconductor processing, worked for NTK Technical Ceramics, Sunnyvale, in 1996-1997, and after that he joined AIT Inc., Torrance, CA, 1997 - 2002, where he developed tooling and process for calibration of electron beam optics, measurements of temperature and mechanical properties of MEMS device. His work with electron beam optics resulted in a US Patent 6,140,657: "Sterilization by Low Energy Electron Beam".

**Susanne Douglas** is staff scientist in the Astrobiology Research Element at JPL. Susanne received her PhD in Geomicrobiology from University of Guelph, Guelph, Ontario, Canada in 1993. Prior to joining JPL, she held post-doctoral research positions at the department of Geology, University of Toronto, and at the department of microbiology, University of Guelph, from May 1993 to May 1994, and from June 1994 to June 1995, respectively, and a Contract Assistant Professorship, Dept. of Microbiology, U. of Guelph, from Jan 1996-Aug 1998. Susanne co-authored over 20 papers published in refereed journals in the area of geomicrobiology.

**Thomas George** is the Supervisor of the MEMS Technology Group at the In situ Technology and Experiments Systems



Section at JPL. He invented the concept of a pump-less microfabricated electron microscope and is a co-inventor with J. Feldman and J. Z. Wilcox of the AEXS instrument. He received his PhD in Materials Science from the University of California at Berkeley (UCB). Prior to

joining JPL he worked on the transmission electron microscopy of semiconductor materials as a postdoctoral researcher at UCB and Intel Corporation, as well as the the Nagoya Institute of Technology, Japan. He joined JPL in 1990, where he set up and operated an HRTEM laboratory and managed tasks aimed at the development of AlGaN-based, solar-blind, ultraviolet detectors. He has successfully commercialized a JPL-developed, bulk Si-micromachined tunneling infrared detector. He currently manages the MEMS Technology Group with diverse MEMS-based projects and has also initiated and manages programs aimed at the development of the AEXS and a Force Detected NMR microinstrument for planetary exploration. He has authored/co-authored over 40 archival journal publications and holds 4 U.S. patents.



**Jason Feldman** was a member of the engineering staff at the In situ Technology and Experiments Systems Section at JPL. He received his BA in Physics from the University of California at Berkeley. At Lawrence Berkeley National Laboratory, he worked with Professor Paul Richards on the Millimeter Anisotropy

Experiment (MAX). In addition to design, fabrication, and implementation of high speed radiation-hard serial data communications systems for a high altitude NASA-NSBF balloon-borne telescope, he was responsible for setting up a new laboratory and calibration facility, optimization of the analog electronics, and coordination of systems compatibility with collaborators. He joined Caltech in 1998 as an assistant engineer and JPL in 1999. He co-invented the Atmospheric Electron X-ray Spectrometer with T. George and J. Z. Wilcox, was the cognizant engineer for the Patch Plate dust adhesion experiment, and for the Cryobot Active Thermal Probe development project.